

Development of a Technique for In-Flight Jet Noise Simulation – Part II

R. Mani*

General Electric Corporate Research and Development, Schenectady, N. Y.

W. S. Clapper† and E. J. Stringas‡

General Electric Aircraft Engine Business Group, Cincinnati, Ohio
and

G. Banerian§

NASA Headquarters, Washington, D. C.

The present paper describes the results of a theoretical study aimed at relating noise signatures obtained in a freejet facility for simulation of forward flight effects on jet noise with the noise signatures recorded in true flight. An important feature of the paper is extensive theory-data comparison. The transformation is carried out by extracting the "basic directivity" of the noise after correcting for refraction, turbulent scattering, and absorption effects and then employing a suitable multipole source decomposition to evaluate the proper dynamic effect. Detailed directivity comparisons are presented for three primary jet velocities and two flight velocities for the three nozzle types as described in Part I of this paper. It is concluded that the validity of the freejet technique and associated transformation procedure has been satisfactorily demonstrated.

Introduction

THE basic issue addressed in this paper can be explained with the aid of Fig. 1. Shown schematically in that figure is a proposal that has emerged in the past few years for a convenient scheme to evaluate the noise emitted from an exhaust nozzle when the nozzle itself is in relative motion. Loosely speaking, we may describe it as a partial wind-tunnel concept. The primary (small) exhaust nozzle is embedded in the exhaust plume of a much larger, low-velocity exhaust jet flow, whose ideal jet exit velocity is adjusted to be equal to the desired forward flight velocity. Measurements of the noise of this system are carried in a conventional anechoic environment on a large number of microphones located "far" from the system in an entirely stationary environment. These measurements are the conventional acoustic measurements, such as, for example, third-octave SPL spectra. The issue of interest is the transformation that one needs to apply to data acquired in such a facility, in order to be able to deduce the noise signatures that one might expect when the primary exhaust nozzle itself translates to the left at a certain flight velocity.

Some comments are in order on the parameter limits that were of interest to the present authors concerning the size of the secondary jet, primary nozzle type, etc. Our concern was primarily with situations where the freejet (secondary jet) to primary jet area ratio was of the order of 50:1. Since we were very much concerned with acquiring as much as possible of inlet arc data, it was necessary to displace the exhaust plane of the primary nozzle considerably aft of the exhaust plane of the secondary nozzle (as shown schematically in Fig. 1). Flight simulation in the velocity range of 0–300 fps were of primary interest. A paramount consideration of interest was that the transformation procedure developed be completely in-

dependent of primary exhaust nozzle type, primary exhaust nozzle velocity and temperature, and whether the primary nozzle exhaust flow contained shocks or not. It was also considered essential for the transformation to be valid over a wide frequency range of practical interest, e.g., from 250 Hz to 10 kHz full size and over a wide range of angles. (With θ_1 denoting the angle measured from the engine inlet axis, one is normally interested in jet noise emitted in the range $30 \text{ deg} \leq \theta_1 \leq 160 \text{ deg}$.) Finally, the transformation ought to work with the type of data acquired in conventional jet noise measurements, e.g., SPL spectra at various fixed microphones. Phase information, for example, is conspicuously not provided by such data and would, in any event, probably not be very meaningful in jet noise.

Before concluding this section, it is worthwhile to stress that one paramount requirement must be met if the simulation technique is to have any prospects of success. This is that we must assume that a large area ratio exterior flow does suffice to simulate the alteration of the aerodynamics of the exhaust flow (both the steady and unsteady aspects of it) due to relative velocity in the same manner as occurs in flight. In other words, the source alteration for all conceivable mechanisms of jet noise (such as jet mixing noise, shock noise, lip noise) due to flight is assumed to be adequately simulated by the imposition of the freejet relative velocity.

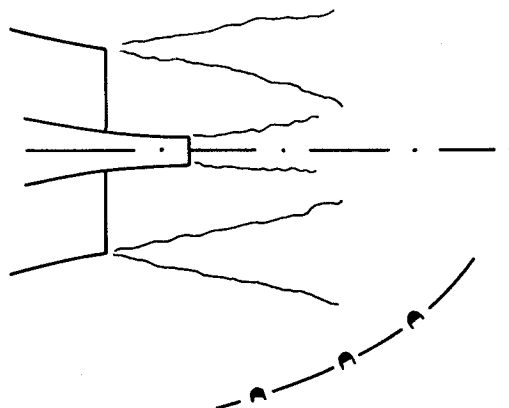


Fig. 1 Schematic of the problem.

Presented as Paper 76-532 at the 3rd AIAA Aeroacoustics Conference, Palo Alto, Calif., July 20-23, 1976; submitted Oct. 12, 1976; revision received April 27, 1978. Copyright © American Institute of Aeronautics and Astronautics, Inc., 1976. All rights reserved.

Index categories: Noise; Aeroacoustics; Testing, Flight and Ground.

*Manager, Engineering Mechanics Program. Member AIAA.

†Manager, High Velocity Jet Noise Technology. Member AIAA.

‡Manager, Jet Noise Technology. Member AIAA.

§Chief, Noise and Pollution Reduction Branch. Member AIAA.

Also, the transformation cannot cope with the situation if different, significant internal noise sources occur in the scale model experiments with a freejet, as opposed to full-scale flight experiments. There is in fact no rigorous procedure of verifying such assumptions and one has to resort to estimates of internal noise mechanisms, mean velocity profile estimates or measurements, etc., to check the validity of such assumptions.

Development of Analytical Transformation

Screening Study

In this section, we will examine some theoretical aspects of various approaches that have been suggested for carrying out the required transformation. At the outset, it is pertinent to note that as long as measurements in the freejet facility are confined to conventional far-field measurements (in the sense of SPL spectra measurements on a fixed set of microphones on a given arc or sideline far from the freejet), and if the freejet to primary nozzle area ratio is of the order of 50:1 or so, there is no absolutely defensible, perfectly rigorous procedure of carrying out this transformation. The reason is that, in general, for a given frequency band, the transformation must depend on the type of sources producing the flight noise, and there is no unique procedure of estimating such source distributions from measurements of sound pressure levels alone in the far field. Purely from the point of view of the acoustics of a parallel shear flow, neglecting effects of turbulence, freejet divergence, etc., a transformation procedure independent of source type can be developed and shown to be valid at asymptotically high frequencies. However, both because freejets of area ratio 50:1 (offset so that their exhaust plane is upstream of the nozzle exhaust plane) do not provide a nonspreading parallel shear flow environment over the source regions of the primary exhaust nozzle and because turbulence scattering absorption effects are not small at high frequencies, such transformation procedures, based on wave propagation in steady laminar parallel shear flow, are not as useful as one might hope. For completeness, we will briefly indicate the basics of this approach and also how it has fared in attempts to apply it to experimental data.¹⁻³ The freejet is assumed to provide an acoustic environment corresponding to a parallel flow, doubly infinite jet. In fact, most investigations have gone a step further and treated the parallel flow jet as a slug flow jet.^{1,2} Investigators have first sought to answer the question of what noise signature would be produced by the same distribution of sources in an acoustic environment where the "jet" flow is now a parallel slug flow of infinite radius, i.e., an infinitely large wind tunnel (with the microphones now immersed in the wind). We first wish to examine under what conditions, even assuming the freejet flow to be able to provide a nondivergent parallel shear flow environment extending from upstream infinity to downstream infinity independent of axial location, "transformations" can be rendered independent of source type or source frequency. (Parenthetically, we note that once this transformation from "freejet" to true wind-tunnel environment is achieved, it is a trivial matter to rigorously transform from the wind-tunnel frame to the flight condition, since the flight frame of reference is related to the wind-tunnel frame by a straightforward Galilean transformation.)

For purposes of such a screening study, it is instructive to examine theoretical solutions for typical point singularities in the situations of flight and in a freejet. In the freejet, the results depend on the frequency, flow profile, and location of the source. At low frequencies, we assume a plug flow model; at high frequencies, a parallel sheared flow is assumed. Only asymptotic low- and high-frequency limits are presented. Also, we assume the sources to be located on the jet centerline (see Fig. 2a).

The flight results are quite well-known and frequency independent, so we will first state the freejet results. The plug

flow results can be derived, based on the development given in Ref. 4, while the parallel shear flow results are based on Ref. 5. It is reiterated that only the asymptotic low- and high-frequency results are given; i.e., for the plug flow model only the leading term of an asymptotic expansion as the frequency tends to zero is given and, conversely, for the parallel shear flow model, only the leading term in an asymptotic expansion as the frequency tends to infinity is given.

1) Pressure source:

$$p' \sim \frac{1}{R[1 - M \cos(\theta_{FJ})]^2} \quad (1a)$$

at low frequencies

$$p' \sim \frac{1}{R[1 - M \cos(\theta_{FJ})]} \quad (1b)$$

at high frequencies (outside the zone of silence).

Note that M is the flight Mach number, θ_{FJ} the angle in the freejet measured from the jet exhaust axis, and R the radius of measurement.

2) xx quadrupole:

$$p' \sim \frac{\cos^2 \theta_{FJ}}{[1 - M \cos(\theta_{FJ})]^2} \quad (2a)$$

at low frequencies

$$p' \sim \frac{\cos^2(\theta_{FJ})}{[1 - M \cos(\theta_{FJ})]} \quad (2b)$$

at high frequencies (outside the zone of silence).

3) xr quadrupole:

$$p' \sim \frac{2 \cos(\theta_{FJ}) \sin(\theta_{FJ})}{[1 + (1 - M \cos \theta_{FJ})^2]} \quad (3a)$$

at low frequencies

$$p' \sim \frac{\cos(\theta_{FJ}) \sqrt{(1 - M \cos \theta_{FJ})^2 - \cos^2 \theta_{FJ}}}{(1 - M \cos \theta_{FJ})} \quad (3b)$$

at high frequencies (outside the zone of silence).

4) rr quadrupole:

$$p' \sim \frac{2 \sin^2(\theta_{FJ})}{[1 + (1 - M \cos \theta_{FJ})^2]} \quad (4a)$$

at low frequencies

$$p' \sim \frac{[(1 - M \cos \theta_{FJ})^2 - \cos^2 \theta_{FJ}]}{(1 - M \cos \theta_{FJ})} \quad (4b)$$

at high frequencies and outside the zone of silence.

The results for x and r dipoles are not given explicitly and can easily be deduced from the preceding equations.

The high-frequency results have been given outside the zone of silence. Inside the zone of silence, they would all be modified by an exponential attenuation factor (for p') as:

$$\exp\left(-k \int_0^{r_0} f dr\right) \quad (5)$$

where

$$f(r) = |(1 - M(r) \cos \theta_{FJ})^2 - \cos^2 \theta_{FJ}|^{1/2}$$

and r_0 is uniquely defined (depending on θ_{FJ}) as the radius at which $f(r_0) = 0$. $k = \omega/c$ where ω is the source frequency in rad/s and c is the speed of sound.

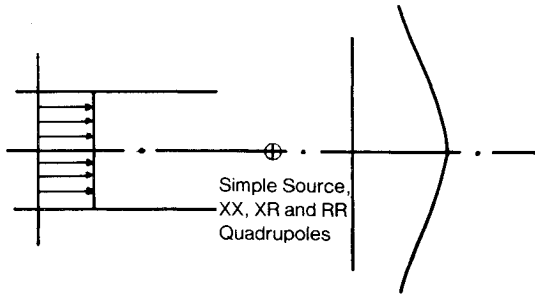


Fig. 2a Velocity profiles used for analytical low- and high-frequency solutions.

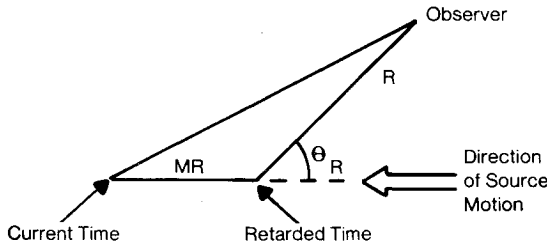


Fig. 2b Illustrating the retarded coordinates used in the flight solutions.

In terms of a similarly retarded radius R and retarded angle θ_R , the corresponding flight results (frequency independent) are (see Fig. 2b):

1) Pressure source:

$$p' \sim \frac{I}{R(1 + M \cos \theta_R)} \quad (6)$$

2) xx quadrupoles:

$$p' \sim \frac{\cos^2(\theta_R)}{(1 + M \cos \theta_R)^3} \quad (7)$$

3) xr quadrupoles:

$$p' \sim \frac{\sin(\theta_R) \cos(\theta_R)}{(1 + M \cos \theta_R)^3} \quad (8)$$

4) rr quadrupoles:

$$p' \sim \frac{\sin^2(\theta_R)}{(1 + M \cos \theta_R)^3} \quad (9)$$

The zone of silence for the freejet of Fig. 2a is the region $0 \leq \theta_{FJ} \leq \cos^{-1}[1/(1 + M)]$.

One approach to the problem of transforming freejet data to wind-tunnel conditions may be explained as follows.^{1,2} The freejet is assumed to be large enough relative to the primary jet such that the evolution of plane waves from the source region is complete, and also large enough so that the outgoing part of these plane waves is assumed to be the same as if the primary jet were in a wind tunnel. Then this outgoing wave will: 1) be refracted at the interface of the freejet and still air and 2) suffer some form of transmission amplification or loss as it negotiates the freejet/still-air interface.

To take account of the refractive effect, we may expect the signal emerging at θ_{FJ} in the freejet experiment to correspond to one emerging at a lesser angle, θ_R , in the flight case, where θ_{FJ} and θ_R are related by

$$\cos \theta_{FJ} = \frac{\cos \theta_R}{1 + M \cos \theta_R} \quad (10)$$

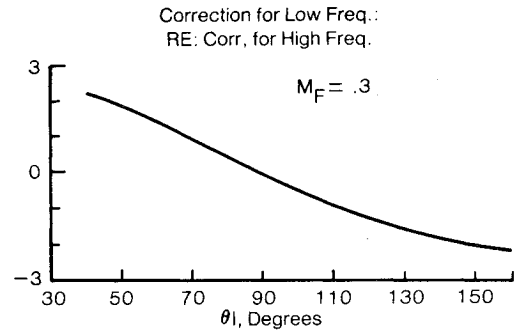


Fig. 3a Frequency dependence of amplitude correction.

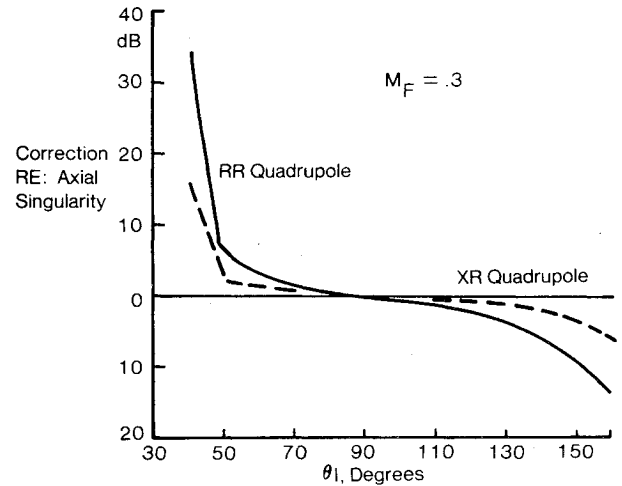


Fig. 3b Dependence of amplitude correction on singularity type at asymptotically low frequencies.

It is a characteristic feature of such methods^{1,2} that no use is made in these methods of freejet data within the zone of silence [i.e., no real value of θ_R is related to θ_{FJ} for the preceding relation for $\theta_{FJ} < \cos^{-1}[1/(1 + M)]$ and, conversely, no real value of θ_{FJ} corresponds to $\theta_R > \pi - \cos^{-1}[1/(1 + M)]$ and also one-to-one correspondence between freejet and flight data cannot be used to infer flight data for $\theta_R > \pi - \cos^{-1}[1/(1 + M)]$.

To take account of the second effect, Ref. 1 uses the Ribner-Miles^{6,7} solution to the problem of transmission of plane waves across a vortex sheet to infer the transmission coefficient. The net result is a procedure to correct freejet data to flight by means of an angle shift formula, as expressed by the Ribner-Miles solution.¹ The resulting amplitude correction formula by such methods is frequency or source-type independent and generally calls for applying a negative correction (in dB) in the exhaust arc freejet data ($\theta_R \leq 90$ deg) and a positive correction (in dB) to the inlet arc freejet data to correct it to flight. Since Eqs. (1-4) are frequency dependent while Eqs. (6-10) are not, it is clear that the transformation cannot be strictly frequency independent. Also, even considering Eqs. (1-4), we note that the frequency dependence is itself source-type dependent and hence the transformation cannot be rigorously source-type independent either. Figure 3 emphasizes this need for accounting for frequency and source-type dependence by: 1) showing the amplitude correction needed to transform freejet data to flight at asymptotically low frequencies relative to that at asymptotically high frequencies for a fixed singularity type, namely axial singularities such as pressure sources, x dipoles and xx quadrupoles; and 2) by showing the correction for transverse singularities relative to those for axial singularities at asymptotically low frequencies.

TURBULENT MIXING STUDIES

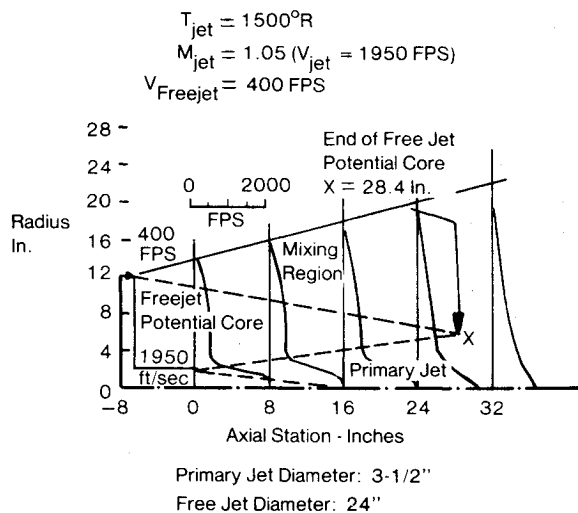


Fig. 4 Computed velocity profiles for GE freejet facility.

A second approach to the transformation problem is also possible based on the following philosophy. As illustrated in Fig. 4, it is arguable that, with freejet to primary nozzle area ratios of 50 or so and with the freejet exit plane displaced upstream of the primary nozzle exit plane (to enable acquisition of inlet arc data), what the freejet achieves is a proper simulation of the relative velocity environment insofar as simulation of the primary nozzle plume aerodynamics does but very little of the acoustic simulation of uniform flow over the sources. Of course, at extremely shallow angles to the jet exhaust axis, we may expect an acoustic impact of the freejet in the sense of a refractive effect. Based on this notion, one may first attempt a transformation of the freejet data to a static frame somewhat analogous to the manner in which Ribner's group⁸ sought to separate jet noise directivity into a combination of refractive, convective, and "basic" directivity effects. Once such a "static" directivity has been extracted, we can attempt a static-to-flight transformation. This, again, cannot be accomplished without attempting to say something about the nature of the sources. The next section will give the details of this source decomposition procedure. This was the approach adopted in the present study.

Recommended Procedure

The recommended procedure for transformation of freejet noise to flight noise is as follows. Using the measured freejet data, we first extract from it a "static" directivity, which is the directivity that the sources associated with the primary nozzle plume as altered by the effect of the relative wind would create if they radiated into a static rather than the freejet environment. We next use this basic directivity pattern to estimate what the noise in flight would be.

To retrieve the basic directivity, we first subtract the refractive effect of the freejet flow. At low frequencies (for $k_0 a \leq 3$), the plug flow model solution for a point pressure source is used to make this correction.⁴ For $k_0 a \geq 3$ in the inlet arc, the asymptotic high-frequency solution for a pressure source, namely $p'_{FJ} \sim (1 - M \cos \theta)^{-1}$, is employed to subtract the refractive effect. For $k_0 a \geq 3$ in the exhaust arc, a suggestion of Schubert⁹ was used to deduce the refractive effect. Previous jet noise work based on a comparison of results from Ref. 4 (which employs a plug flow model) and those from Ref. 5 (which develops a high-frequency theory for parallel sheared flow) has shown that $k_0 a = 3$ approximately delineates the upper limit of applicability of a

⁴ k_0 is the usual wave number of the noise and a is the radius of the freejet.

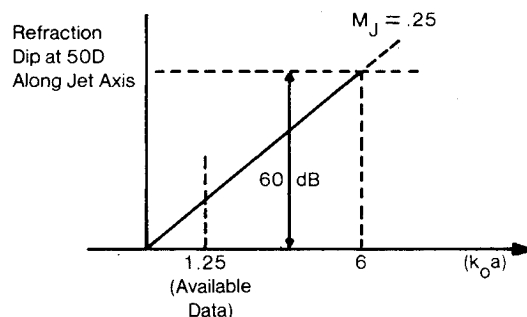


Fig. 5a Illustrating refraction saturation due to scattering by turbulence.

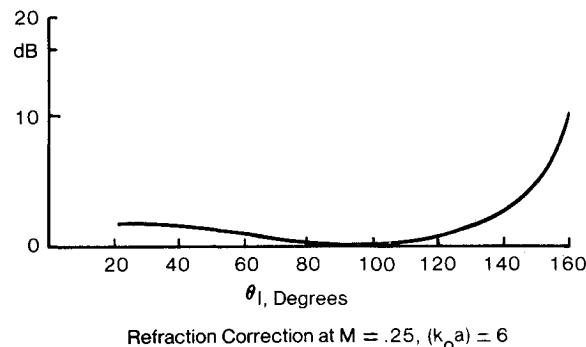


Fig. 5b Example of refraction correction.

plug flow model. Schubert has suggested that one first determine the refractive effect along the jet exhaust axis as a refractive dip on jet axis proportional to freejet Mach number times the frequency parameter ($k_0 a$). He then suggests that a shape factor essentially independent of frequency and Mach number be employed to deduce the refraction at any other angle. Actually, this shape factor is shown by Schubert to be dependent on the radius of measurement (this dependence arises from jet spread), but for $\theta_j \geq 20$ deg, which is the only regime for which we use these ideas, the shape factor is substantially independent of radius of measurement. This procedure was adopted for $3 \leq k_0 a \leq 6$ using the experimental data taken by Ribner and his students with point sources in jets.¹⁰ Actually the data are available only for $k_0 a \leq 1.25$ and, hence, a linear extrapolation of it for $k_0 a \geq 1.25$ but less than 6 was used. The test data from our freejet experiments showed a tendency for the refractive dip to saturate, presumably due to turbulent scattering, beyond $(k_0 a)$ greater than 6. This was inferred by examining, for example, the difference between the SPL's at $\theta_j = 40$ deg and $\theta_j = 20$ deg. Such a difference (at given jet Mach number) does not increase indefinitely with $k_0 a$ but was found to level off for $k_0 a \geq 6$. The refractive correction for the exhaust arc was, therefore, taken independent of $(k_0 a)$ for $(k_0 a) \geq 6$ though still linearly proportional to the freejet Mach number (Fig. 5a).

The precise equations employed to account for the refraction effect in the exhaust arc ($20 \text{ deg} \leq \theta_j \leq 90 \text{ deg}$) are as follows. For $3 \leq k_0 a \leq 6$, the correction at $\theta_j = 20$ deg is taken as $(7(k_0 a)M)$ dB where M is the freejet Mach number. The correction at $\theta_j = 30, 40, 50$, and 60 deg are taken as equal to that at 20 deg divided by 2, 4, 6, and 8 (based on data shown in Fig. 2 of Ref. 10). No correction is applied for $\theta_j = 70, 80$, and 90 deg. Also, if $(k_0 a)$ exceeds 6, only the correction at $k_0 a = 6$ was used. An example of the estimated refraction effect at $M = 0.25$ and $k_0 a = 6$ is shown in Fig. 5b.

One additional propagation effect of the freejet needs to be accounted for. This relates to the fact that fine-grained turbulence in the shear layer of the freejet can absorb sound especially at high frequencies. Crow has given a theory¹¹ for this effect which indicates that this results in an effective

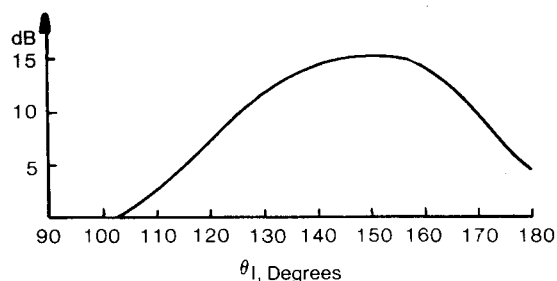
absorption coefficient proportional to frequency (and freejet Mach number)². Based on the path lengths that the sound has to traverse through the freejet, we deduced how this absorption mechanism would vary with θ_j . A recent experimental study¹² has, in fact, demonstrated such absorption effects for the case of plane sound waves impinging normally on turbulent jets. Landahl¹³ has also pointed out that in considering "the propagation of an infinitesimal wave in a flow with pre-existing fluctuations one may speculate that the fluctuations will act qualitatively like an eddy viscosity." He suggested that the eddy viscosity might be eighty times as effective as the molecular viscosity and this estimate was assumed herein to be valid at $M=0.12$ and 20 kHz to establish the constant of proportionality in Crow's expression. There is, at the present time, no independent experimental justification for this choice of the constant of proportionality. The attenuation due to the molecular viscosity in air at 20 kHz (the "classical" absorption) is about 1.4 dB per 100 feet, and based on Landahl's suggestion and path length considerations, the following expression was used to account for this effect. The absorption in dB was taken as equal to $(0.83) \cdot M^2 \cdot k_o a \cdot (2.8 - \theta_j/50)$ with θ_j in degrees. This expression was not used for $\theta_j > 140$ deg since, as Fig. 4 indicates, the turbulent shear layer paths for sound waves traveling at such large angles to the jet exhaust axis are small enough to prevent significant absorption.

Having subtracted the refractive and absorptive effects of the freejet as previously described, we are still faced with the task of predicting the noise that would be produced in flight by such a source distribution. An extended source distribution yields in the far field for each frequency band a certain directivity pattern. To predict the noise distribution that such a pattern would produce in flight, we proceed as follows. We attempt to synthesize the "static" directivity data in each frequency band by a combination of nozzle fixed point singularities determined by the following criteria:

1) Since no phase information is available in the far-field SPL measurements (and would probably not be very meaningful in the jet noise situation), we attempt a synthesis with *uncorrelated* point singularities. The jet provides an axis of symmetry and, hence, it is natural to seek the point singularities as a combination of axial and radial singularities. In other words, we assume the noise field in a given frequency band to be generated by a set of singularities F_o, F_x, F_y , etc.; i.e., that the sound field is a solution to

$$\nabla^2 p + k_o^2 p = F_o \delta(x) \delta(y) \delta(z) + F_x \delta'(x) \delta(y) \delta(z) + F_y \delta(x) \delta'(y) \delta(z) + \dots$$

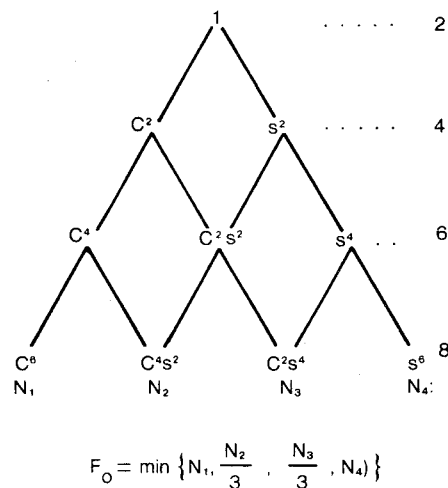
where the point is that F_o, F_x, F_y , etc. are assumed to be mutually uncorrelated so that they contribute to the far-field mean-square pressure only additively. An example is given in Fig. 6 of how a certain combination of a radial dipole, axial



$$\langle F_r^2 \rangle + 3 \langle F_a^2 \rangle + 285 \langle Q_{xxr}^2 \rangle$$

- A Synthesis of Exhaust Arc Noise by a Combination of Uncorrelated Singularities

Fig. 6 Example of synthesis of exhaust arc noise.



Reset $(N_1 - F_o), (N_2 - 3F_o), (N_3 - 3F_o), (N_4 - F_o)$, Etc.

Fig. 7 Singularity "tree" used in source decomposition.

dipole and a fourth-order singularity (all mutually uncorrelated) can be employed to synthesize an exhaust arc radiation pattern characterized by a 15 dB convection falloff, a 10 dB refraction dip, and peaking at $\theta_j = 150$ deg. Because the mean-square pressure of any such singularity is symmetric about both $\theta = 0$ deg and $\theta = 90$ deg, it is necessary to synthesize both the inlet and exhaust arc noise separately.

2) As shown in Fig. 7, an issue of uniqueness arises, since due to relations such as $[1 = \cos^2 \theta + \sin^2 \theta]$, the pressure pattern of a pressure source can be synthesized from that of a sum of equal transverse and radial dipoles, etc. As indicated on the right side of Fig. 7, the dynamic exponent required to derive the flight result associated with each level of the singularity "tree" varies with the level of the singularity. Hence, the following singularity fitting procedure was adopted. We first decide on a level of fitting using the criterion that the data ought to be reconstructed, on the average, to within an error of 2 dB. Any hidden symmetries in the singularity distribution, however, is detected by a recombination procedure indicated in Fig. 7. What is meant by this is the following. Let us say that a non-negative combination of octupoles N_1, N_2, N_3 , and N_4 (each with characteristic mean-square pressure directives as $\cos^6 \theta, \cos^4 \theta \sin^2 \theta, \cos^2 \theta \sin^4 \theta, \sin^6 \theta$, respectively) suffices to fit the measured "basic" directivity data (either for the inlet or the exhaust arc) to within an average error of less than 2 dB. To recover the hidden pressure monopole in this distribution, we examine the least of the numbers $N_1, N_2/3, N_3/3, N_4$. This determines F_o . We then derive new numbers M_1, M_2, M_3, M_4 as $M_1 = N_1 - F_o, M_2 = N_2 - 3F_o, M_3 = N_3 - 3F_o, M_4 = N_4 - F_o$, etc. F_1 (the coefficient in the "tree" of $\cos^2 \theta$) is now determined as the least of $M_1, M_2/2$ and M_3 and F_2 of $M_2, M_3/2$ and M_4 , and so on. We are employing here an intuitive notion that the data ought to be reconstructed with the least singular distribution of uncorrelated sources possible.

Even with these simplifications, it is necessary to solve a least-squares problem of the type—"find \bar{x} to minimize $\|\bar{A}\bar{x} - \bar{b}\|$ subject to a non-negativity constraint $\bar{x} \geq 0$." This exercise was carried out using an algorithm based on the Kuhn-Tucker theorem of optimization theory.¹⁴ If the criteria that the reconstruction be carried out with the least-singular mix of uncorrelated axial and radial singularities and that the reconstruction be accurate to an average error of 2 dB are accepted, the resulting reconstruction is unique. This is because both the solution to the non-negative least-squares problem and the recombination problem illustrated in Fig. 7 are unique.

¹⁴ In Fig. 7, c stands for $\cos \theta$ and s for $\sin \theta$.

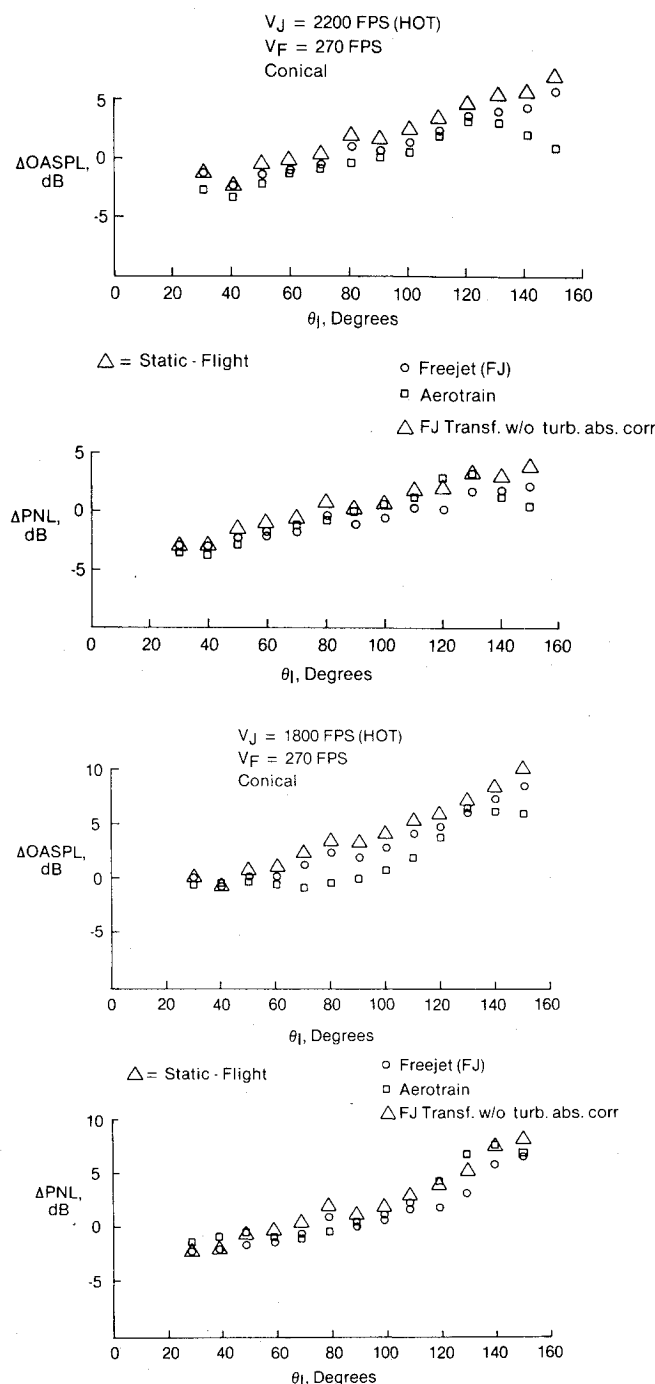


Fig. 8 Conical nozzle noise: OASPL and PNL comparisons on a difference basis.

The procedure just mentioned was coded into a computer program which proceeds as follows. The input data are a frequency parameter ($k_o a$), SPL versus directivity data, and the freejet or flight Mach number. The directivity data are first corrected for refraction and absorption by turbulence in a manner dependent on M and ($k_o a$). Commencing from the top of the tree of Fig. 7, using the algorithm based on the Kuhn-Tucker theorem, a non-negative least-squares fit of the data till the data are fitted to an average error < 2 dB is carried out. The singularities are recombined to yield the least-singular distribution fitting the data. This final distribution is then employed with the correct dynamic exponent appropriate to each singularity level to predict the directivity pattern in each Doppler shifted frequency band. It is important to note that the source reconstruction procedure is only used to infer the "dynamic effect" appropriate to each

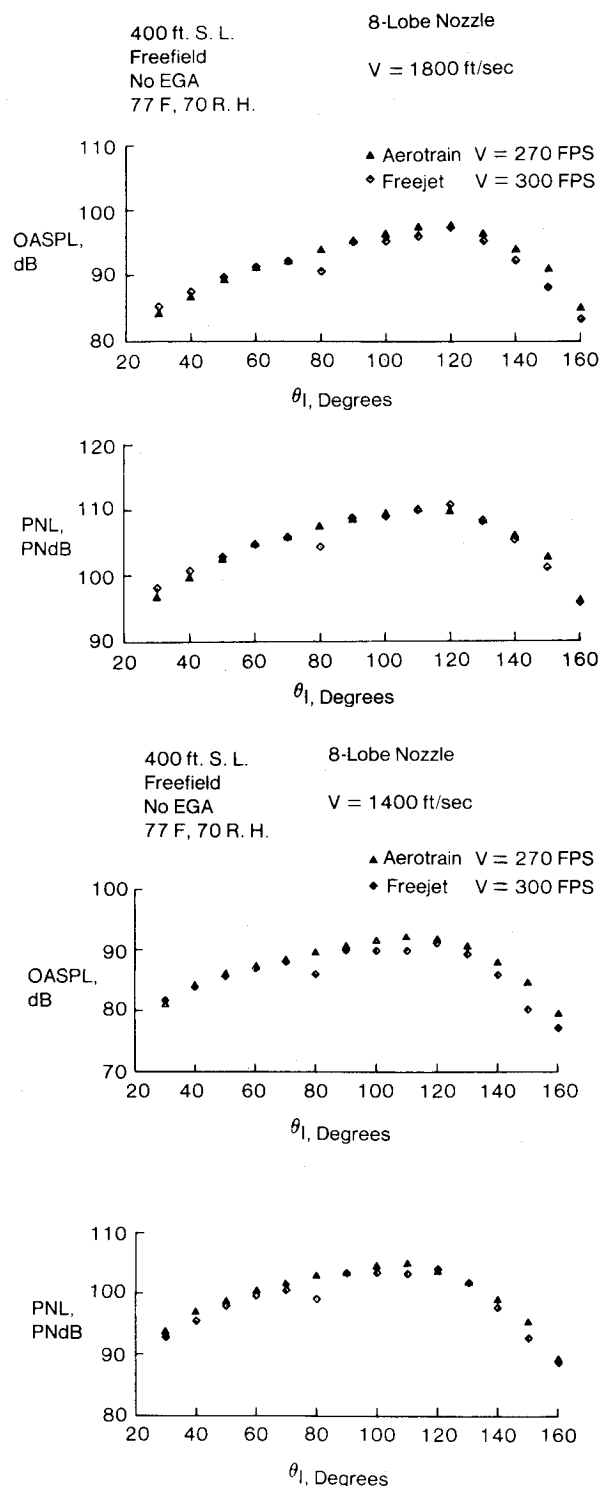


Fig. 9 Eight-lobe daisy nozzle noise: OASPL and PNL comparisons.

narrow band directivity pattern with the dynamic effect correction itself being applied to actual freejet data corrected for refraction and turbulence absorption.

Discussion of Results

Figures 8-11 summarize the results of the study. Before discussing them, one preliminary remark concerning the results of the source decomposition study is in order. We first wish to reiterate that the source decomposition, as used in the present study, is only an apparent reconstruction and represents some amalgam of the way in which refractive and convective effects, various mechanisms of jet noise such as mixing noise, shock noise, and lip noise collectively manifest

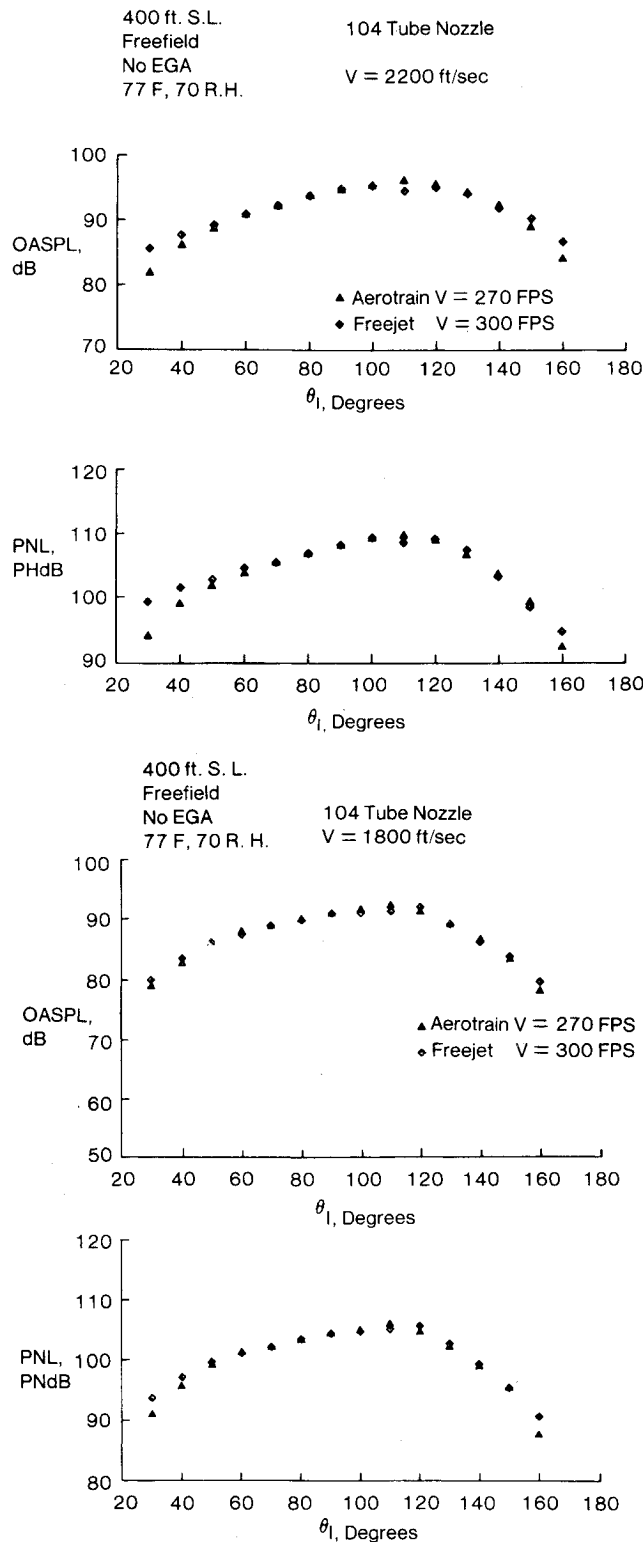


Fig. 10 104 tube multitube suppressor nozzle noise: OASPL and PNL comparisons.

themselves. Having expressed this disclaimer that the relationship of the apparent source reconstruction used in this paper to the physics of the processes producing flight jet noise is somewhat tenuous, we would like to mention that for conical nozzle noise, the source decomposition does suggest that exhaust arc noise is primarily quadrupole in character, especially at low frequencies. At higher frequencies, the exhaust arc "basic" directivity is often amenable to decomposition by just (uncorrelated) dipole singularities. Conversely, the low-frequency inlet arc noise often requires

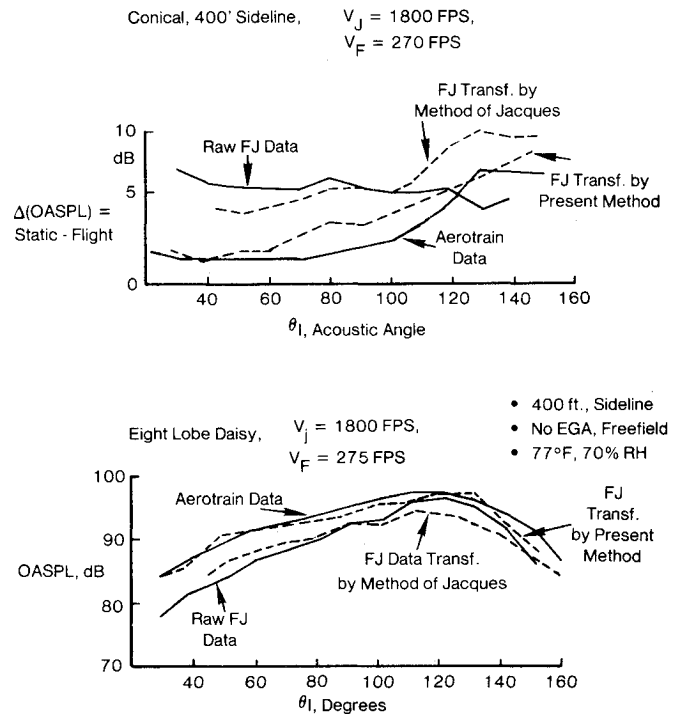


Fig. 11 Comparisons of flight data with freejet data transformed by the method of Ref. 2 and with untransformed freejet data.

only dipoles to adequately synthesize. The high-frequency inlet arc noise often required the use of quadrupole singularities to achieve the desired level of curve fitting (i.e., to an average error of less than 2 dB).

Although all the freejet data of the entire program were transformed (for all the three nozzles at all the combinations of primary and flight velocities tested) and compared with results from the Aerotrain program, limitations of space preclude our showing all these comparisons and, hence, in Figs. 8-11, we confine ourselves to a representative sampling of such comparisons, only on an integrated basis (i.e., comparisons are only shown for the OASPL and PNL).

From a practical point of view, the OASPL and PNL directivity are indeed of greatest interest. However, since the current transformation procedure is completely frequency dependent—not just because the refraction and turbulence absorption corrections are frequency dependent, but also because the effective dynamic effect exponent to be applied to the directivity in each third-octave band depends on the sources needed to synthesize that directivity pattern—one has to first transform each third-octave band separately and then sum up the contributions in the usual manner to derive OASPL's and PNL's.

Such integrated directivity comparisons are shown in Figs. 8-10. The data labeled as "freejet" are the freejet data *scaled and transformed*. For the conical nozzle (as Part I of this paper points out), there were problems with static scaling itself and hence the comparisons are shown on a difference basis; i.e., the change in noise going from the static case to the flight case is compared for the Aerotrain and freejet experiments. For the suppressor nozzles, since static scaling holds up extremely well, absolute levels are compared. The figures speak for themselves and certainly no systematic difficulty is evident. We observe that the agreement is poorest for the conical nozzle though still quite acceptable.

In view of the ad hoc and empirical deduction of the constant of proportionality used in applying Crow's theory (Ref. 11) in Fig. 8; i.e., for the conical nozzle, the comparisons are also shown as obtained by neglecting entirely the turbulence absorption correction. Because of the shorter path lengths involved in the inlet arc, neglecting this correction has

a smaller impact on the inlet arc than on the exhaust arc. The OASPL comparisons are worsened somewhat, while the PNL comparisons appear somewhat improved.

Finally, we address the issue of how the methods contained in Refs. 1 and 2 would work when applied to the data of Part I. Jacques' method² was adopted since it deals directly with a cylindrical freejet geometry. We first checked that our coding of this method was correct by obtaining complete agreement with a worked example given in Fig. 4.35 (p. 155) of Ref. 2. Comparisons are shown both for a conical nozzle and an eight lobe nozzle in Fig. 11. It is clear (as also reported in Ref. 3) that these methods tend to underestimate the measured flight noise by as much as 3-5 dB.

Conclusion

The principal conclusion of this study is that, following the sequence of steps of first deriving an equivalent "static" directivity by accounting for refraction and turbulence absorption in a semiempirical manner and then employing a source decomposition procedure tailored to broadband jet exhaust noise to derive the flight results, a rational transformation procedure for obtaining flight-type data from a static but wind-on freejet experiment can be developed. Extensive theory-data comparisons for the entire program described in Part I were carried out and highlights of these have been presented herein. Considering the various sources of data error, particularly in the moving frame experiment, the procedure is considered to have been adequately validated over a wide combination of flight and jet velocities as well as exhaust nozzle types.

Acknowledgments

This study was supported by the Federal Aviation Administration under Contract DOT-OS-30034 with R. Zukerman as Project Monitor. We would be remiss if we did not acknowledge the tremendous benefit derived from conversations with our colleague T. F. Balsa in the course of our study. In particular, he provided the high-frequency analytic solutions employed in the section entitled "Screening Study."

References

- ¹Amiet, R.K., "Correction of Open Jet Wind-Tunnel Measurements for Shear Layer Refraction," *Progress in Astronautics and Aeronautics*, Vol. 46, edited by I. R. Schwartz, AIAA, New York, 1976, pp. 259-280.
- ²Jacques, J. R., "The Noise from Moving Aircraft; Some Relevant Models," Ph.D. Thesis, University of Cambridge, U.K., Aug. 1975.
- ³Packman, A.B., Ng, K.W., and Paterson, R.W., "Effect of Simulated Forward Flight on Subsonic Jet Exhaust Noise," *Journal of Aircraft*, Vol. 13, Dec. 1976, pp. 1007-1013.
- ⁴Mani, R., "The Influence of Jet Flow on Jet Noise. Part I: The Noise of Unheated Jets," *Journal of Fluid Mechanics*, Vol. 73, Part 4, 1976, pp. 753-778.
- ⁵Balsa, T.F., "The Far Field of High Frequency Convected Singularities in Sheared Flows, With an Application to Jet Noise Prediction," *Journal of Fluid Mechanics*, Vol. 74, Part 2, 1976, pp. 193-208.
- ⁶Ribner, H.S., "Reflection, Transmission and Amplification of Sound by a Moving Medium," *Journal of the Acoustical Society of America*, Vol. 29, 1957, pp. 435-441.
- ⁷Miles, J.W., "On the Reflection of Sound at an Interface of Relative Motion," *Journal of the Acoustical Society of America*, Vol. 29, 1957, pp. 226-228.
- ⁸MacGregor, G.R., Ribner, H.S., and Lam, H., "'Basic' Jet Noise Patterns after Deletion of Convection and Refraction Effects: Experiments vs. Theory," *Journal of Sound and Vibration*, Vol. 27, 1973, pp. 437-454.
- ⁹Schubert, L.K., "Numerical Study of Sound Refraction by a Jet Flow. II. Wave Acoustics," *Journal of the Acoustical Society of America*, Vol. 51, 1972, pp. 447-463 (see especially p. 459).
- ¹⁰Atvars, J., Schubert, L.K., and Ribner, H.S., "Refraction of Sound from a Point Source Placed in an Air Jet," *Journal of the Acoustical Society of America*, Vol. 37, 1965, pp. 168-170.
- ¹¹Crow, S.C., "Viscoelastic Character of Fine Grained Isotropic Turbulence," *Physics of Fluids*, Vol. 10, July 1967, pp. 1587-1589.
- ¹²Takaku, I. and Horiuchi, T., "Attenuation of Low Frequency Sound in a Turbulent Duct," *Journal of the Acoustical Society of America*, Vol. 58, 1975, pp. 916-919.
- ¹³Landahl, M.T., "A Wave-Guide Model for Turbulent Shear Flow," *Journal of Fluid Mechanics*, Vol. 29, Part 3, 1967, pp. 441-459.
- ¹⁴Lawson, C.L. and Hanson, R.T., *Solving Least Squares Problems*, Prentice-Hall, Englewood Cliffs, N.J., 1974, Chap. 23.